Effects of Light Quenching on the Emission Spectra and Intensity Decays of Fluorophore Mixtures

Ignacy Gryczynski,[1] Józef Kuśba,[2] and Joseph R. Lakowicz[1,3]

We examined a series of fluorophore mixtures to determine the wavelength selectivity of light quenching and the effects of light quenching on the emission spectra and intensity decays. Light quenching can be accomplished using a single excitation pulse train and quenching wavelength (one-beam) or with longer-wavelength quenching pulses time-delayed relative to the excitation pulses (two-beam). Both one-beam and two-beam light quenching were found to alter the intensity decays of the mixtures. The frequency-domain intensity decay data were analyzed to reveal the fractional intensity of each fluorophore in the mixture and the effects of light quenching on the fractional contribution of each fluorophore to the total intensity. Fluorophores were selected to provide a range of decay times and emission wavelengths. The extent of quenching in the mixtures was dependent on which fluorophore had the higher radiative decay rate and emission intensity at the quenching wavelength. A general theory is presented which describes the intensity decays in terms of the extent of quenching of each fluorophore and the time delay between excitation and quenching pulses. The effects of light quenching on the fractional intensities of each fluorophore in the mixture, recovered from the intensity decay analysis, were found to be in quantitative agreement with that predicted from steady-state measurements of light quenching and from the spectral properties of the fluorophores. The data on light quenching of mixtures demonstrate that light quenching may be used for selective quenching of fluorophores and thus of potential value for studies of multichromophoric systems.

KEY WORDS: Light quenching; emission spectra; intensity decays; fluorophore mixtures.

INTRODUCTION

The emission from polymers and biological macromolecules is frequently complex due to the presence of two or more emitting species. Resolution of the multicomponent emission is often obtained from the effects of collisional quenchers. For example, fluorophores on the surfaces of proteins are typically accessible to water-soluble quenchers, while interior fluorophores are not quenched by acrylamide or iodide.[1,2] Similarly, fluorophores localized in the acyl side-chain region of membranes can be quenched by hydrophobic quenchers but not by water-soluble quenchers.[3] Collisional quenching, combined with time-resolved measurements, have provided insights into the solution properties of biomolecules.[4,5]

[4] Abbreviations used: 3AF, 3-aminofluoranthene; DA, Dansylamide or 5-dimethylaminonaphthalene-1-sulfonamide; DCM, 4-(dicyanmethylene)-2-methyl-6-(p-dimethylaminostyryl)-4H-pyrane; DCS, 4-dimethylamino-4'-cyanostilbene; DMF, dimethylformamide; DMSO, dimethylsulfoxide; EB, ethidium bromide; ErB, erythrocin B; FD, frequency domain; LQ, light quenching; RhB, rhodamine B; R6G, rhodamine 6G; [Ru(bpp)₃]²⁺, ruthenium tris(1,10-bipyridyl).
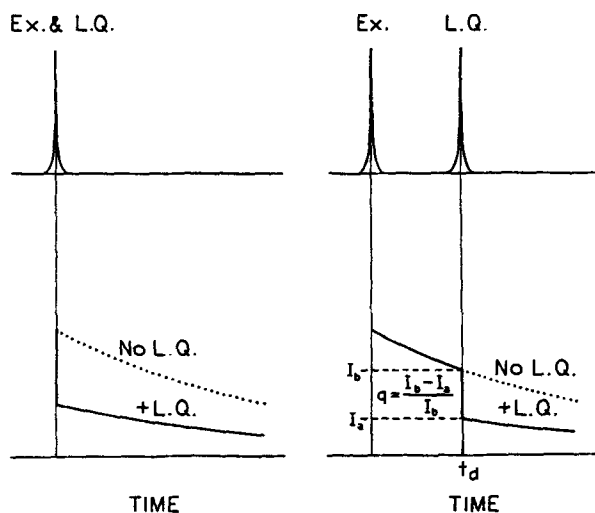
Scheme I. Intuitive description of one-beam and two-beam light quenching.

Collisional quenching is not without its disadvantages. The number of known fluorophore–quencher pairs is limited, so that a suitable quencher is not always available. Collisional quenching requires molecular contact between the fluorophore and the quenchers.[6] Consequently, it is necessary to dissolve reasonable quantities of the quencher so that it can diffuse to and quench the fluorophores during the excited state lifetime. Hence, collisional quenching occurs only in relatively fluid solvents where translational diffusion is rapid. Also, the fluorophore must be exposed to the phase containing the dissolved quenchers. Additional requirements for a useful collisional quencher include the absence of significant light absorption by the quencher at the excitation and emission wavelengths and that the macromolecular structure not be perturbed by the quencher.[7,8]

Because of these considerations we chose to examine light quenching as an alternative to collisional quenching. The factors governing light quenching are expected to be distinct and complementary to collisional quenching. In recent reports we described the use of long-wavelength illumination as a method to decrease the excited-state population.[9–12] The basic idea is to illuminate the sample with wavelengths overlapping the emission spectrum. This causes stimulated emission which occurs parallel to the direction of the long-wavelength quenching beam. With the usual right-angle observation the intensity is decreased, and hence we use the phrase "light quenching" to describe the phenomenon of fluorescence quenching by stimulated emission. Fluorescence depletion by stimulated emission and transient stimulated emission pumping have recently been

used to study intramolecular vibrational redistribution in small molecules[13] and ozone photodissociation,[14] to control excited-state kinetics,[15] and in series of papers by Zewail's group on real-time probing of chemical reactions.[16–18] In the present report we demonstrate that light quenching can be used for selective quenching in mixtures of fluorophores. Selective quenching is demonstrated by changes in the emission spectra and multiexponential intensity decays from fluorophore mixtures. The relative extent of quenching of each component in the mixture was found to be predictable based on steady-state measurements of light quenching or the spectral properties of the fluorophores.

THEORY

One- and Two-Beam Light Quenching

Two types of light quenching experiments are possible with pulsed excitation (Scheme I). Light quenching can occur with a single pulse and single wavelength (left), which both excites and quenches the sample. We refer to such experiments as one-beam light quenching. One-beam light quenching requires excitation on the long-wavelength absorption edge of the fluorophore so that the excitation wavelength overlaps the emission spectrum of the sample. Such experiments require careful selection of the fluorophores and wavelengths but are technically simple since only a single laser beam is required.

Light quenching can also be accomplished with a second longer-wavelength pulse train, which is typically time-delayed relative to the pulsed excitation. Such experiments are referred to as two-beam light quenching. Upon arrival of the quenching pulse at time $= t_d$, one expects a nearly instantaneous decrease in the intensity due to a decrease in the excited state population (Scheme I, right). For two-beam light quenching one can adjust the wavelength and time delay (t_d) of the quenching pulse. The instantaneous extent of quenching (q) is given by the intensity before (I_b) and after (I_a) the quenching pulse

$$q = \frac{I_b - I_a}{I_b} \tag{1}$$

For the present experiments we examined mixtures containing two fluorophores, each of which displays a single-exponential decay in the absence of light quenching. A general theory for light quenching is complex and must consider the effects of the delay time (t_d), which

for nonzero values results in oscillations in the frequency-domain data.[10] This general theory for light quenching of mixtures, on which our analysis programs are based, is provided in the Appendix. For the experiments presented in this paper we used either one-beam light quenching or a short delay time (t_d) so that oscillations were not very significant.[10] Additionally, the use of a short delay time results in little contribution to the signal from emission occurring prior to the quenching pulse. That is, the emission occurs almost completely after the quenching pulse. Hence, to a first approximation the observed intensity decay can be represented as a sum of exponentials in which the preexponential factors represent the fractional contribution of each fluorophore to the intensity decay. However, we found during the analyses that to obtain a satisfactory description of the decay, the emission occurring in our experiments prior to the quenching pulses has to be taken into account.

Intensity Decays in the Absence and Presence of Light Quenching

In the present paper the delay times are short relative to the decay times of the fluorophores. Also, the chosen fluorophores displayed single-exponential decays in the absence of light quenching. Hence, we could use the multiexponential model for an exact description of the one-beam light quenching experiment and as an approximate description of the two-beam light quenching of the mixtures. The intensity decay is described by

$$I(t) = \sum_i \alpha_i e^{-t/\tau_i} \qquad (2)$$

where α_i are the amplitudes of the components with decay times τ_i. The fractional contribution of each component to the steady-state intensity is given by

$$f_i = \frac{\alpha_i \tau_i}{\sum_j \alpha_j \tau_j} \qquad (3)$$

The parameters describing the multiexponential decays were determined by least-squares analysis of the frequency-domain data.[19,20]

Since each fluorophore displays different extents of light quenching, the relative contributions of the fluorophores to the intensity decay will be altered by light quenching. Suppose that each fluorophore (i) is quenched by a factor Q_i, where

$$Q_i = F_{0i}/F_i \qquad (4)$$

and F_{0i} and F_i are the steady-state intensities of the fluo-

rophore in the absence and presence of light quenching, respectively. By steady-state intensity we mean the average value observed with continuous illumination by a train(s) of laser pulses. Then the fractional intensities of the ith species in the absence (f_i^0) and presence (f_i) of light quenching are given by

$$f_i^0 = \frac{\alpha_i^0 \tau_i}{\sum_j \alpha_j^0 \tau_j} = \frac{f_i^0}{\sum_j f_j^0} \qquad (5)$$

$$f_i = \frac{f_i^0/Q_i}{\sum_j f_j^0/Q_j} \qquad (6)$$

Suppose the intensity decay of a two-component mixture is measured in the absence and presence of light quenching. The value of f_i^0 and f_i can be used to calculate the relative amount of quenching of each fluorophore. More specifically, for a two-component mixture, use of Eq. (6) yields

$$\frac{Q_1}{Q_2} = \frac{f_1^0 f_2}{f_2^0 f_1} \qquad (7)$$

We use the f_i^0 and f_i values from the multiexponential analysis to recover the ratio Q_1/Q_2. These values were compared with separate measurements of Q_1 and Q_2 from steady-state quenching experiments performed under the same experimental conditions.

Cross Sections for Light Quenching

The sensitivity of a fluorophore to light quenching is described by the cross section for light quenching. This cross section is given by

$$\sigma_{lq} = \frac{C}{\tau_N} \frac{I(\lambda)}{\int I(\lambda) \, d\lambda} = \frac{C k_r I(\lambda)}{\int I(\lambda) d\lambda} \qquad (8)$$

where C is a constant, τ_N is the radiative lifetime, and $I(\lambda)$ is the amplitude of the emission spectrum at the quenching wavelengths λ.[21,22] Since τ_N is the inverse of the radiative decay rate k_r, the extent of light quenching is expected to be proportional to the radiative rate. Also, if the quenching wavelength is centered on the emission maximum, fluorophores with narrow emission spectra are expected to display more light quenching than those with a broad emission. For purposes of estimating the relative cross section we used the peak-normalized emission spectra on the wavelength scale $[I(\lambda)]$ and divided the maximum intensity by the integrated area $[\int I(\lambda)d\lambda]$.

The natural lifetime or radiative decay rate can be calculated from the measured lifetime (τ) and quantum yield (Φ). These values are given by

$$\tau = \frac{1}{k_r + k_{nr}} \qquad (9)$$

$$\Phi = \frac{k_r}{k_r + k_{nr}} \qquad (10)$$

where k_{nr} is the sum of the nonradiative decay rates. Hence, the radiative rate is given by

$$k_r = \frac{\Phi}{\tau} \qquad (11)$$

The cross section for light quenching can be related to the steady-state fluorescence intensities in the absence (F_0) and presence (F) of quenching[23,24] by

$$Q = \frac{F_0}{F} = 1 + \sigma_{lq} t_p P \qquad (12)$$

where t_p is the pulse width of the quenching pulse and P is the power density. It is difficult to measure directly the values of σ_{lq} because of difficulties in knowing the precise shape and power of the quenching pulse. However, the relative values of σ_{lq} can be estimated from the extents of quenching of each fluorophore. If Q_1 and Q_2 are known from steady-state measurements, then the relative cross sections σ_1 and σ_2 can be obtained from

$$\frac{Q_1 - 1}{Q_2 - 1} = \frac{\sigma_1}{\sigma_2} \qquad (13)$$

MATERIALS AND METHODS

One-Beam Light Quenching

The experimental arrangements are different for one-beam and two-beam light quenching. For the one-beam experiments, excitation and light quenching are due to the same incident beam. In order to obtain overlap of the excitation with the emission spectrum, it is necessary to excite the sample on the extreme long-wavelength edge of the absorption spectra. We use an experimental arrangement similar to that used previously for one-beam light quenching.[24] A rhodamine 6G (R6G)[4] dye laser tunable from 565 to 615 nm was synchronously pumped by the 514-nm output of a mode-locked argon ion laser. The pulse width was near 5 ps, the repetition rate was 3.795 MHz, and the average power was about 100 mW. This light was focused to a spot size of about 20 μm in diameter, resulting in a maximum intensity of about 2×10^9 W/cm². Without focusing, the spot size was about 2 mm in diameter. The emission was selectively observed from the focal region
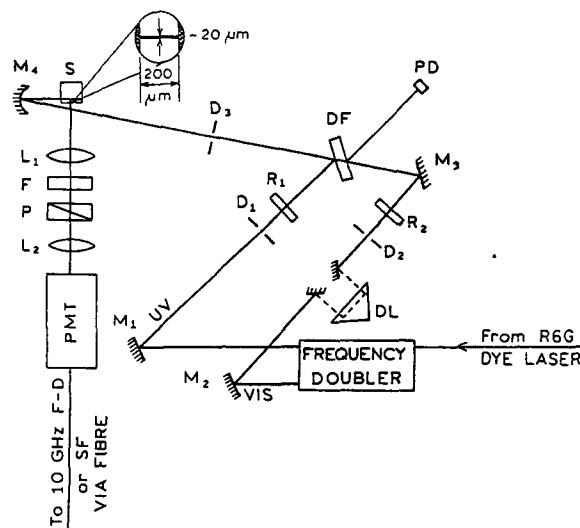
Scheme II. Experimental arrangement for two-beam light quenching.

of the illuminated sample using a spatial filter (air slit) 3 mm high and 200 μm wide (Scheme II). The fluorophore concentrations used in one-beam experiments were typically in the range 10^{-4}–10^{-5} M and were adjusted to provide approximately equal fluorescence signals from each component at the observation wavelength. It should be noted that in one-beam light quenching the excitation is within the red edge of the absorption band, where absorption is very low.

The excitation was polarized vertically, as occurs from the output of our dye laser. The emission was observed through a filter, which transmitted light at the desired wavelengths. For intensity measurements the emission polarizer was 54.7° from the vertical. Control measurements using the solvent without the fluorophores gave signals less than 0.5% of the solution emission, for all polarization conditions and excitation (quenching) wavelengths.

Time-resolved intensity measurements of mixtures in one-beam experiments were analyzed using the multiexponential model [Eq. (2)]. The recovered fractional intensities f_i^0 and f_i were used to calculate the ratio Q_1/Q_2 [Eq. (7)]. In the Appendix we show that both f_i and the ratio Q_1/Q_2 can be found simultaneously [see Eqs. (A33)–(A35)].

Two-Beam Light Quenching

The experimental arrangement for two-beam light quenching was described previously.[10,11] The light source was again the R6G dye laser, but in this case the frequency-doubled output at 285 nm was used for ex-
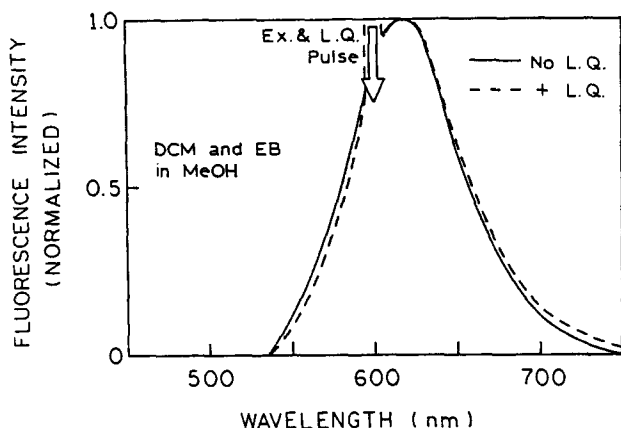
Fig. 1. Emission spectra of a mixture of DCM and EB in methanol without (—) and with (---) one-beam light quenching at 600 nm.

citation, and the fundamental output at 570 nm was used for light quenching (Scheme II). The average power at 285 and 570 nm was about 5 and 150 mW, respectively. The region of overlap of the excitation and quenching beams was selectively observed with the 3 mm × 200-μm spatial filter. The time delay between the excitation and the quenching pulses was approximately 20 ps for all experiments, a delay which was found to result in the largest amount of quenching. The concentrations of fluorophores used in two-beam experiments, about 5 × 10^{-6} M, were adjusted to provide approximately similar fluorescence signals from nonquenched mixture components at the observation wavelength.

Intensity and anisotropy decay measurements were obtained using frequency-domain (FD) instrumentation described previously.[25,26] For intensity decay measurements the excitation was vertically polarized and the emission observed through a polarizer 54.7° from the vertical. Analysis of the FD intensity decay data for two-beam light quenching was accomplished using the model described in detail in the Appendix. This model includes instantaneous jump at $t = t_d$ (Scheme I). Equations (A38)–(A40), which were used to fit our experimental data, contain six variable parameters; f_1^0, τ_1, τ_2, t_d, q_1, and q_2. In our analysis the two lifetimes (τ_1 and τ_2) and t_d were held fixed and f_i^0, q_1, and q_2 were fitted parameters.

RESULTS

Light Quenching with Similar Emission Spectra

Emission spectra are shown in Fig. 1 for a mixture of   4-(dicyanomethylene)-2-methyl-6-(p-dimethylami-

nostyryl)-4H-pyrane (DCM) and ethidium bromide (EB). The excitation and quenching wavelength was near 600 nm, which overlapped with the emission spectra of both fluorophores. The emission spectra of DCM and EB are similar, so that one does not expect a spectral shift with light quenching, and no spectral shift was observed (Fig. 1). We present only the normalized emission spectra for such one-beam light quenching experiments. In a one-beam experiment, excitation and quenching occur simultaneously, and a direct comparison of the intensities with and without light quenching is not possible.

The extent of light quenching, or cross section for light quenching, is expected to be proportional to the radiative decay rate. We chose DCM and EB because of their different decay times in methanol, 1.22 and 5.80 ns, respectively. The lifetime of EB can be as large as 21 ns,[27] suggesting a considerably smaller radiative rate for EB than for DCM. Hence, we expected DCM to be quenched to a greater extent than EB at comparable illumination intensities.

Since the emission spectra of DCM and EB are similar, the relative contribution of each fluorophore in the absence and presence of light quenching cannot be determined from the emission spectra (Fig. 1). Hence we measured the intensity decays of the DCM–EB mixture using the frequency-domain method. At low excitation intensities, where light quenching is not significant, the intensity decay is a double exponential (Fig. 2; top). The fractional intensities of each component were recovered from the least-squares analysis and are summarized in Table I. The f_i values reveal nearly equal contributions of both fluorophores at the observation wavelength of 660 nm: f(DCM) = 0.527 and f(EB) = 0.473. As the excitation intensity is increased, the frequency response changes (Fig. 2, bottom). The shift toward a lower frequency suggests an increased contribution of the longer-lived EB in the presence of light quenching. This impression is confirmed by the least-squares analysis (Table I), which indicates that EB now contributes about 75% to the emission [f(EB) = 0.747] while the DCM contribution has decreased to 25% [f(DCM) = 0.253].

The relative amplitudes in the presence of light quenching can be used to calculate the extent of quenching of each fluorophore in the mixture. More specifically, the value of Q_1/Q_2 can be obtained from Eq. (7). From the intensity decay analysis of the DCM–EB mixture (Table I), the ratio is 3.38 (Table II). As expected, DCM, with its higher quantum yield and higher radiative decay rate, is quenched to a greater extent than EB.

In a separate steady-state experiment we measured the extent of quenching of each fluorophore (Table III).
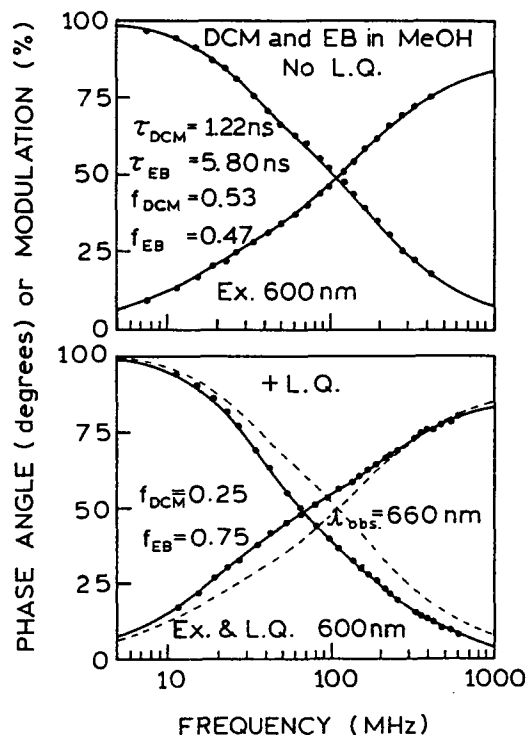
Fig. 2. Frequency-domain intensity decay of the DCM-EB mixture without (top) and with (bottom) light quenching. The dashed line (lower panel) is the frequency response of the unquenched mixture.

These measurements were performed under the same experimental conditions, and in the same instrument, as the frequency-domain intensity decays. The value of $Q = F_0/F$ for DCM and EB were found to be 4.5 and 1.3, respectively. Once again, the short-lived DCM, with its higher radiative decay rate, displayed more quenching than EB. The ratio of the extents of quenching found from the steady-state data (3.46) is in close agreement with that found from the time-resolved data (Table II).

Light Quenching with Different Emission Spectra

We next examined a mixture of erythrocin B (ErB) and rhodamine B (RhB). The emission spectra of these fluorophores are distinct (Fig. 3). The absorption spectra and extinction coefficients of these fluorophores are similar, so that their natural lifetimes and radiative rates are also similar (Table III). Hence, this pair of molecules allows us to test whether the extent of light quenching depends on overlap of the quenching wavelength with the emission spectra of the fluorophore. Emission spectra of the ErB-RhB mixture are shown in Fig. 3 (bottom). Excitation and light quenching at 580 nm results in a blue shift of the emission spectrum. This result is ex-

pected based on the stronger overlap of the quenching wavelength with the emission of RhB and less overlap with the shorter wavelength emission of ErB.

To quantify the relative contributions of ErB and RhB we measured the frequency-domain intensity decays (Fig. 4). The contributions of each fluorophore are easily visible in the unquenched frequency response (top) due to the different decay times, 0.08 and 1.58 ns for ErB and RhB, respectively. In contrast to the previous mixture (Fig. 2), light quenching results in a dramatic shift of the frequency response to higher frequencies (Fig. 4), indicating an increased contribution of the shorter-lived ErB in the presence of light quenching. The relative contributions of ErB and RhB were recovered from the frequency-domain data (Table I). Without light quenching, ErB contributed about 55% of the observed emission. With light quenching the contribution of ErB increases to 79%, indicating relatively more light quenching of RhB than ErB. As for the previous mixture, the individual decay times were not altered by light quenching (Table I).

It is of interest to compare the relative amounts of light quenching of ErB and RhB with the amplitudes of these emission spectra at the quenching wavelength. The amplitudes of the intensity-normalized spectra at the quenching wavelength are 0.95 and 0.27, respectively. Assuming equal radiative rates for ErB and RhB, one expects RhB to be quenched 3.5-fold more strongly than ErB. Use of intensity decay parameters (Table I) and Eq. (14) indicates that RhB is quenched 2.7-fold more strongly than ErB. This value is in good agreement with the ratio (3.08) calculated from the steady-state quenching. These results indicate that for fluorophores with similar radiative rates, the relative extents of quenching can be accurately predicted from the amplitudes of the emission spectra at the quenching wavelength.

Light Quenching with Different Emission Spectra and Decay Times

We next examined two fluorophores with very different decay times and different radiative decay rates. The chosen fluorophores were RhB and ruthenium tris(1,10-bipyridyl), [Ru(bpy)$_3$]$^{2+}$, where the decay times are 1.58 and near 350 ns, respectively. Based on the quantum yields of RhB (0.48) and [Ru(bpy)$_3$]$^{2+}$ (0.02), the radiative decay rates are about 3 × 10^8 and 6 × 10^4 s^{-1}, respectively (Table III). Because of its low radiative decay rate, the extent of light quenching for the Ru complex is expected to be negligible compared with that for RhB.

Table I. Two-Exponential Analysis of Intensity Decays of Mixtures in the Absence and Presence of One-Pulse Light Quenching

Mixture[a]	Quenching mode	$f_1{}^b$	f_2	τ_1 (ns)	τ_2 (ns)	χ_R^2
DCM (1.22 ns) + EB (5.80 ns) in MEOH	No. L.Q.	0.53	0.47	1.27	6.11	0.9
	+ L.Q.	0.25	0.75	1.12	5.64	1.0
ErB (0.08 ns) + RhB (1.58 ns) in H_2O	No. L.Q.	0.55	0.45	0.080	1.58	1.1
	+ L.Q.	0.79	0.21	0.078	1.36	3.6
RhB (1.58 ns) + [Ru(bpy)$_3$]$^{2+}$(350 ns) in H_2O	No. L.Q.	0.61	0.39	1.61	469	1.6
	+ L.Q.	0.17	0.83	1.61	398	1.4

[a]The measured lifetimes of single-fluorophore solutions are given in parentheses. These lifetimes do not depend on light quenching.

[b]f_i are steady-state fractional intensities, calculated from $f_i = \alpha_i\tau_i/\Sigma\alpha_j\tau_j$.

Table II. Comparison of Observed and Predicted Relative Quenching for Mixtures

Mixture[a]	Relative quenching (Q_1/Q_2)	
	Steady state[b]	Time-resolve[c]
DCM + EB	3.46	3.38
RhB + ErB	2.70	3.08
RhB + [Ru(bpy)$_3$]$^{2+}$	5.0	7.6
DCS + DA	2.67	3.31
DCS + 3AF	2.38	2.79

[a]The relative values of Q_1/Q_2 are for the first listed fluorophore divided by the second listed fluorophore.

[b]Calculated from the values of Q_i in Table III.

[c]Calculated from intensity decay parameters using Eq. (7). $f_i{}^0$ and f_i are fractional intensities in the absence and presence of light quenching (Tables I and IV).

Table III. Quantum Yields, Decay Times, Radiative Decay Rates, and Quenching Constants of Fluorophores

Probe	Solvent	τ (ns)	Quantum yield[a]	k_r (ns^{-1})	Q^b
DCM	Methanol	1.22	0.38	0.30	4.5
EB	Methanol	5.80	0.06	0.01	1.3
ErB	Water	0.08	0.02	0.25	1.85
RhB	Water	1.58	0.48	0.30	5.0
[Ru(bpy)$_3$]$^{2+}$	Water	350	0.02	0.00006	1.0
DCS	DMF	0.68	0.076	0.11	3.6
DA	DMF	15.4	0.30	0.02	1.35
DCS	DMSO	0.87	0.08	0.09	3.8
3AF	DMSO	11.7	0.32	0.03	1.6

[a]Quantum yields were estimated using DCS in DMF as a reference compound [28].

[b]Values $Q = I_0/I$, where I_0 and I are fluorescence intensities in the absence and presence of light quenching, were measured for the wavelengths indicated in the figures and in Table V.

The single excitation and quenching wavelength was selected so that the amplitudes of the normalized
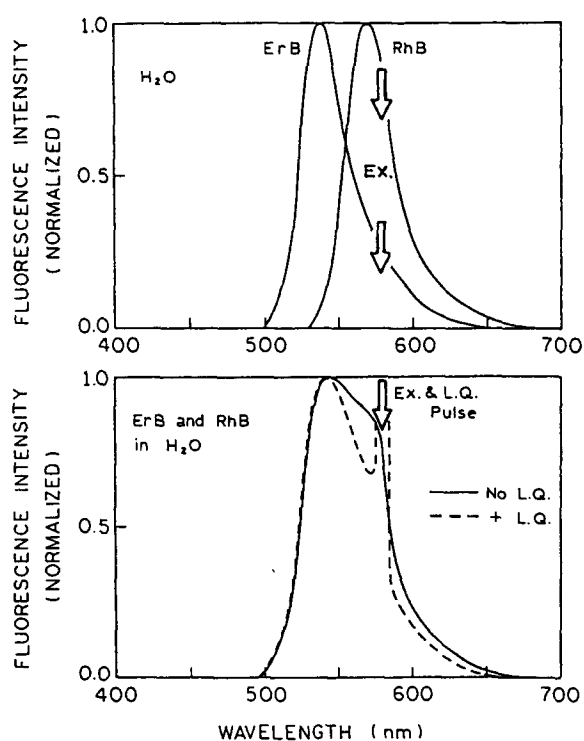
Fig. 3. Emission spectra of ErB and RhB in water (top) and the mixture (bottom) with and without light quenching at 580 nm.

emission spectra were equal (Fig. 5). In the absence of light quenching the emission spectrum is due predominantly to RhB, which displays a narrow emission with a peak near 570 nm (Fig. 5). In contrast, [Ru(bpy)$_3$]$^{2+}$ displays a much broader emission spectrum, with a peak near 600 nm. Light quenching results in a much wider emission spectra (---) than in the absence of light quenching (—), and an increased relative amplitude at longer wavelengths, consistent with an increased fractional contribution of [Ru(bpy)$_3$]$^{2+}$ to the total emission.
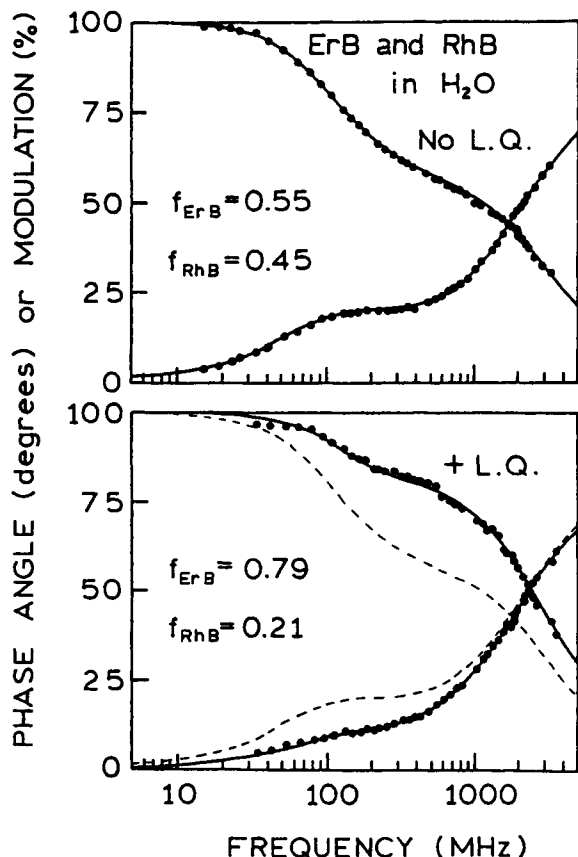
Fig. 4. Frequency-domain intensity decay of ErB–RhB without light quenching (top) and with one-beam light quenching (bottom). The unquenched frequency response in shown as a dashed line in the lower panel. The emission was observed at 550 nm.
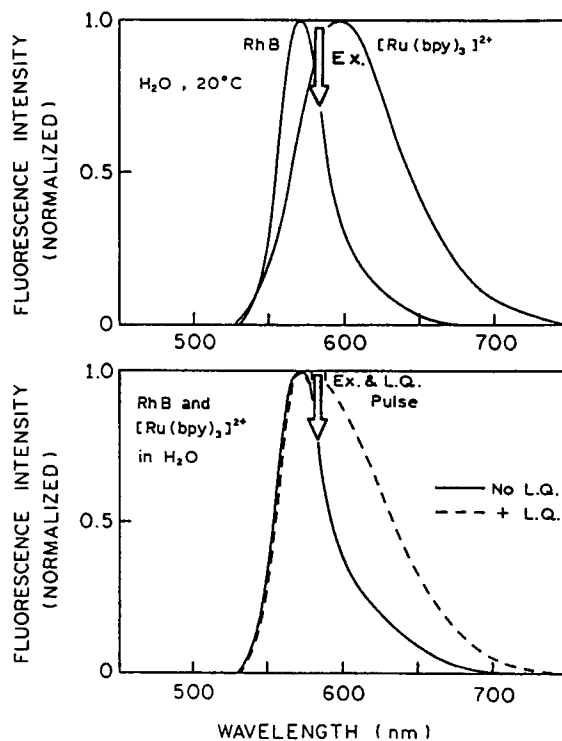

Fig. 5. Emission spectra of RhB and [Ru(bpy)₃]²⁺ in water (top) and the mixture (bottom) with and without light quenching at 580 nm.

The frequency-domain intensity decays were observed at 620 nm. In this case light quenching results in a profound alteration of the frequency response (Fig. 6). The most remarkable feature is the decrease in modulation seen from 4 to 70 MHz. These remarkable changes are the result of a decrease in the fractional contribution of RhB from 0.612 without light quenching to 0.170 with light quenching. Based on the intensity decays we calculated that RhB was quenched 7.6-fold more strongly than [Ru(bpy)₃]²⁺, in good agreement with the measured value of 5.0 (Table II). We note that there was no significant light quenching of [Ru(bpy)₃]²⁺, so that these ratios represent minimum values and the actual ratio may be larger.

Use of Light Quenching as an Indicator of Local Laser Power

The large changes in the frequency response of the RhB–[Ru(bpy)₃]²⁺ mixture led us to investigate the de-

pendence of the emission modulation on excitation power. At an excitation modulation frequency of 22.8 MHz the emission modulation changed by more than fivefold with increasing laser power (Fig. 7). This suggests that the phenomenon of light quenching could be used as a measure of instantaneous power at a site of interest. For instance, it is difficult to know the effective power in a laser scanning confocal fluorescence microscope due to the numerous optical elements. The use of a mixture, such as that shown in Fig. 7, can provide a measure of the local power from the modulation of the emission, which is independent of the total observed intensity.

Two-Beam Light Quenching with Different Emission Spectra

We next examined the effects of two-beam light quenching on a mixture of 4-dimethylamino-4'-cyanostilbene (DCS) and 5-dimethylaminonaphthalene-1-sulfonamide (DA). In the case of two-beam light quenching, it is possible to compare directly the emission spectra in the absence and presence of light quenching by blocking the quenching beam. Light quenching of the DCA–DA mixture results in a decreased ampli-
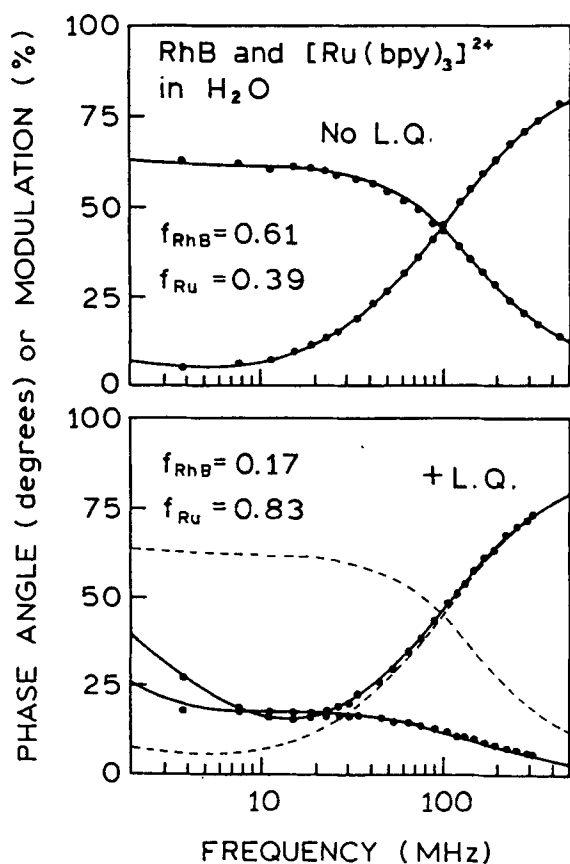
Fig. 6. Frequency-domain intensity decay of the RhB-[Ru(bpy)₃]²⁺ without (top) and with (bottom) light quenching. The emission was observed at 620 nm.
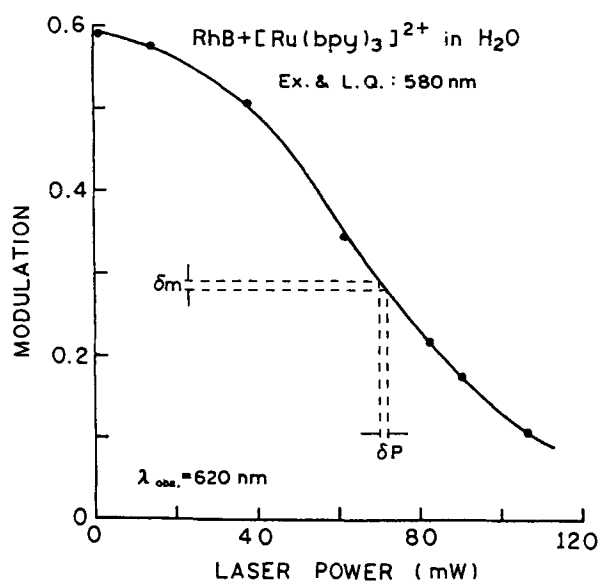

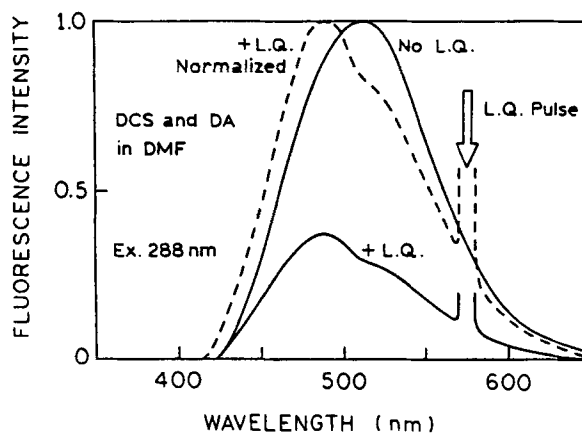Fig. 7. Effect of light quenching on the modulation of the RhB–[Ru(bpy)₃]²⁺ mixture at 22.8 MHz.

Fig. 8. Emission spectra of a mixture of DCS and DA in DMF without and with time-delayed light quenching at 576 nm.

tude which is immediately reversible upon blocking of the 576-nm quenching beam. Normalization of the emission spectra reveals a blue shift upon light quenching (Fig. 8). Since DCS emits at a longer wavelength than DA, these spectra indicate that DCS is preferentially quenched upon illumination at 576 nm.

Frequency-domain intensity decays of the DCS–DA mixture are shown in Fig. 9. Excitation with 288-nm pulses and quenching with a 576-nm pulse delayed by 20 ps results in an increased phase angle and decreased modulation, from 10 to 100 MHz, indicating an increased contribution of the longer-lived DA (15.4 ns) with light quenching. The analysis (Table IV) indicates that the fractional intensity of DA increases from 0.38 to 0.67, whereas the fractional intensity of DCS decreases from 0.62 to 0.33 with light quenching. This is in agreement with longer-wavelength emission and a higher radiative rate constant for DCS relative to DA (Table III). Once again, we calculated the relative amounts of quenching from changes in the intensity decay. These values (Table II) agree with that predicted from the steady-state data. Examination of Fig. 9 reveals that the phase angles decrease above 400 MHz in the presence of light quenching. This effect is due to the time delay between excitation and quenching, which results in an oscillating frequency response.[10]

Two-Beam Light Quenching with Similar Emission Spectra

As a final example of the influence of the radiative decay rate on light quenching, we examined fluorophores with similar emission spectra (Fig. 10), a mixture of DCS and 3-aminofluoranthene (3-AF). The emission
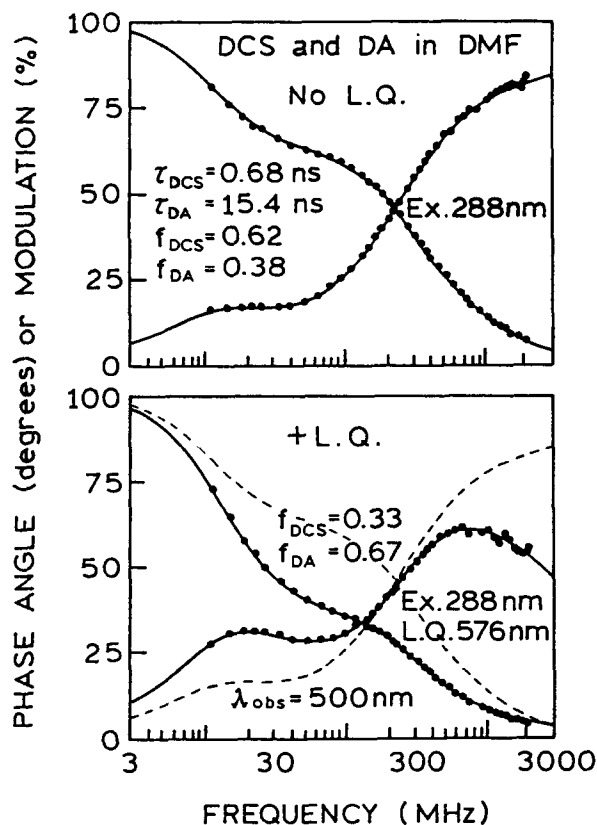
Fig. 9. Frequency-domain intensity decay of DCS–DA without (top) and with (bottom) time-delayed light quenching at 576 nm.

We compared the relative amounts of quenching of DCS and 3AF with those predicted from the radiative rates (Table III). Since the emission spectra are similar, no adjustments are required for spectral shape or overlap of the emission spectra with the quenching wavelength. The extent of quenching from the time-resolved or steady-state measurements was 2.4 or 2.8, respectively. These values are in good agreement with the ratio of the radiative decay rates of 2.4 (Table III).

Calculation of the Relative Cross Section for Light Quenching

Under Theory, we described how the relative amounts of quenching from the frequency-domain data could be used to estimate the relative cross sections for light quenching [Eqs. (12) and (13)]. These relative values calculated from the time-resolved data are summarized in Table V. In Table V we also list the ratios calculated from the lifetimes, quantum yields (Table II), and emission spectra of the fluorophores. The relative values of the quenching cross sections were found to be in good agreement. These results indicate that the extent of light quenching is a readily predicted quantity, which can be estimated from the known spectral properties of fluorophores.

of the DCS-3AF mixture is decreased upon illumination at 576 nm, but there is no spectral shift (Fig. 10). The longer lifetime of 3AF suggests that it will be less sensitive to light quenching than DCS. This prediction is confirmed by the frequency response (Fig. 11) and multiexponential analysis (Table IV).

DISCUSSION

What are the differences and/or potential advantages of light quenching as compared with collisional quenching. Light quenching does not depend on the use of dissolved quenchers and translational diffusion. Hence, light quenching can occur in rigid media or for buried fluorophores which are not accessible to chemical

Table IV. Analysis of Mixture Intensity Decays in the Absence and Presence of Two-Beam Light Quenching

Mixture[a]	Quenching mode	f_1^b	f_2	q_1	q_2	χ_R^2
DCS (0.68 ns) + DA (15.4 ns) in DMF	No. L.Q.	0.62	0.38	⟨0⟩	⟨0⟩	0.9
	+ L.Q.	0.33	0.67	0.796	0.326	2.6
DCS (0.87 ns) + 3AF (11.7 ns) in DMSO	No. L.Q.	0.52	0.48	⟨0⟩	⟨0⟩	0.9
	+ L.Q.	0.28	0.72	0.739	0.257	1.4

[a]The measured lifetimes of single-fluorophore solutions in the absence of light quenching are given in parentheses. These lifetimes were fixed during the analyses. The theoretical model used for intensity decay analysis in the presence of light quenching includes instantaneous jump at $t = t_d$ (Scheme I).

[b]f_i are the steady-state fractions of fluorescence associated with the ith individual species.
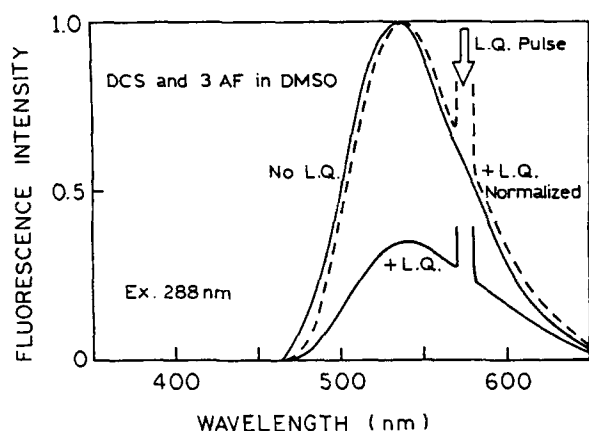
Fig. 10. Emission spectra of a mixture of DCS and 3AF in DMSO in the absence and presence of time-delayed light quenching.
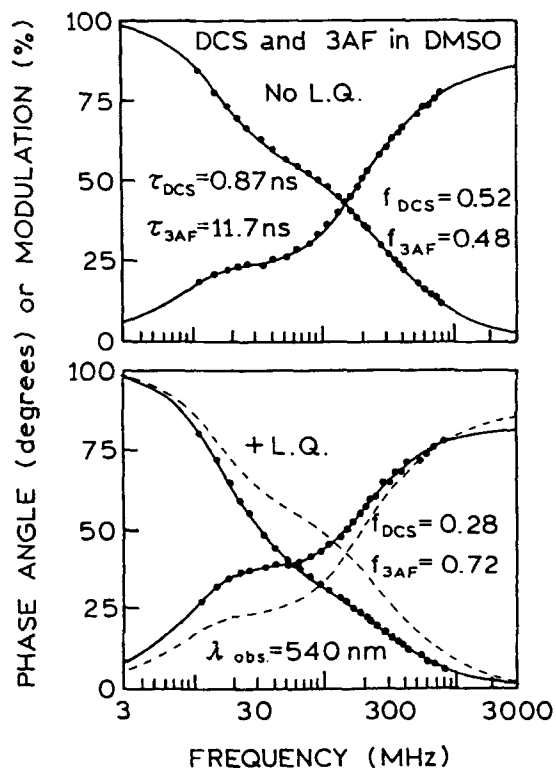

Fig. 11. Frequency-domain intensity decays of DCA–3AF without (top) and with (bottom) time-delayed light quenching at 576 nm.

Table V. Comparison of Predicted and Observed Relative Cross Sections for Quenching

Mixture[a]	λ_q (nm)	Spectral shape factor[b]	Relative cross section for quenching	
			Calculated[c]	Observed[d]
DCM + EB	600	1.0	18.7	11.6
RhB + ErB	580	3.0	3.7	4.7
RhB + [Ru(bpy)₃]²⁺	580	2.0	10,000	>1000
DCS + DA	576	1.5	8.8	7.4
DCS + 3AF	576	1.0	3.9	4.6

[a]The relative values are for the first listed fluorophore divided by the second listed fluorophores.

[b]The fraction of the emission overlapping with the quenching wavelength was calculated from the amplitudes of the emission spectra at the quenching wavelength and the uncorrected emission spectra of the fluorophores.

[c]Calculated from Eq. (8), based on the spectral shift, lifetime, and quantum yields.

[d]The ratio of the cross section was calculated from the ratio $(Q_1 - 1)/(Q_2 - 1)$, where $Q = I_0/I = 1 + \sigma_{lq} \cdot t_p \cdot P$ [23].

not alter the solution conditions of the molecules and thus will not perturb the solution conformation.

A favorable property of light quenching is that the relative effects can be predicted from the spectral properties of the fluorophores. Fluorophores with higher radiative rates are expected to display higher cross sections for light quenching, and by selection of the quenching wavelength one can quench either the solvent-exposed (red shifted) or the solvent-shielded (blue shifted) residues. Additionally, the time delay of the quenching pulse can be adjusted to avoid quenching of fluorophores with short decay times. And finally, the extent of light quenching depends on the orientation of the emission dipole relative to a polarized quenching beam.[12] Consequently, the extent of quenching depends on the time 0 anisotropy of the fluorophore and the extent of rotational motion between polarized excitation and quenching pulses. To the best of our knowledge, collisional quenching has not been shown to depend on fluorophore orientation.

The characteristics of collisional quenching described above are not intended to indicate the superiority of light quenching but, rather, to reveal the complementary characteristics of these phenomena. There can be no doubt about the ease of collisional quenching experiments, which do not require pulsed excitation or laser light sources. In favorable cases it should be possible to use the complementary nature of collisional and light quenching to provide increased information about the solution structure and dynamics of macromolecules.

quenchers. In contrast to chemical quenchers, the light can be reversed by blocking of the quenching beam, rather than more time-consuming dialysis and/or repurification of the sample. Also, the quenching beam does

APPENDIX

Intensity Decay of a Mixture of Fluorophores in the Presence of Light Quenching

We now consider the intensity decay of fluorophore mixtures in the presence of time-delayed light quenching, but the theory can also be applied to one-beam light quenching. Although we experimentally investigated only two-component mixtures, for generality we assume the presence of n components and assume no chemical interaction between the components. In the absence of light quenching the total intensity decay $I^0(t)$ is given by

$$I^0(t) = \sum_k I_k^0(t) = \sum_k J_k^0\, \phi_k^0(t) \qquad (A1)$$

where $I_k^0(t)$ are the intensity decays of the individual components, and J_k^0 and $\phi_k^0(t)$ ($k = 1 \ldots n$) are the steady-state intensities, which are the average intensity with illumination by a pulse train, and the normalized decay functions of the components, respectively. We assume that the intensity decays of the individual components are single exponentials described by the lifetimes τ_k. The decay functions $\phi_k^0(t)$ are then given by

$$\phi_k^0(t) = \frac{1}{\tau_k}\, e^{-t/\tau_k} \qquad (A2)$$

In the presence of light quenching the intensity decays of the components, $I_k(t)$, display an instantaneous decrease at time $t = t_d$ denoting the time of the arrival of the quenching pulse. The intensity decreases may be different for each species and are described by parameters q_k,

$$q_k = \frac{I_{kb} - I_{ka}}{I_{kb}} \qquad (A3)$$

where I_{kb} and I_{ka} are the intensities immediately before and after the quenching pulse, respectively. In the case of one-beam light quenching, I_{kb} denotes the fluorescence intensity of the kth component at $t = 0$ in the absence of light quenching.

In the presence of light quenching the intensity decay of the mixture is described by the expression

$$I(t) = \sum_k I_k(t) = \sum_k J_k^0 Z_k \phi_k(t) \qquad (A4)$$

where the decay functions $\phi_k(t)$ are defined as

$$\phi_k(t) = \begin{cases} \dfrac{1}{Z_k}\dfrac{1}{\tau_k}\, e^{-t/\tau_k}, & 0 \le t \le t_d \\[2mm] \dfrac{1}{Z_k}(1 - q_k)\dfrac{1}{\tau_k}\, e^{-t/\tau_k}, & t > t_d \end{cases} \qquad (A5)$$

with Z_k being normalization factors fulfilling the equation

$$\int_0^\infty \phi_k(t_d)\, dt = 1 \qquad (A6)$$

Note that Eq. (A4) is written so that $I(t) = I^0(t)$ before the arrival of the quenching pulse (for $0 \le t \le t_d$), and simultaneously the decay functions $\phi_k(t)$ fulfill the normalization condition, Eq. (A6). One can see from Eqs. (A5) and (A6) that the normalization factors Z_k are given by

$$Z_k = 1 - q_k\, e^{-t/\tau_k} \qquad (A7)$$

In Eq. (A4) the products $J_k^0 Z_k$ are the steady-state intensities of the components in the presence of light quenching

$$J_k = J_k^0 Z_k \qquad (A8)$$

defined as

$$J_k = \int_0^\infty I_k(t)\, dt \qquad (A9)$$

The amounts of instantaneous quenching [q_k in Eq. (A3)] are typically unknown and can be expressed by the measurable amounts of quenching Q_k, defined as

$$Q_k = \frac{J_k^0}{J_k} \qquad (A10)$$

where Q_k is the ratio of the steady-state fluorescence intensity without (J_k^0) and with (J_k) light quenching. The parameter Q_k is analogous to the ratio F_0/F used in a Stern–Volmer plot, where F_0 and F are the intensities in the absence and presence of collisional quencher, respectively. Equations (A7), (A8), and (A10) imply that

$$Q_k = \frac{1}{Z_k} = \frac{1}{1 - q_k\, e^{-t_d/\tau_k}} \qquad (A11)$$

$$q_k = \left(1 - \frac{1}{Q_k}\right) e^{t_d/\tau_k} \qquad (A12)$$

In the case of one-pulse light quenching, or for a time delay much shorter than the decay time, the exponential term in Eq. (A12) is unity. Then the instantaneous amount of quenching q_k can be readily calculated from Q_k.

In the present paper we characterized the effects of light quenching on the intensity decays of fluorophore mixtures. In this case the extent of quenching of each component is reflected in the fractional intensities f_k,

which represent the fractional contribution of each component to the total measured intensity. These fractional intensities are given by

$$f_k^0 = \frac{J_k^0}{J^0} \quad \text{(A13)}$$

$$f_k = \frac{J_k}{J} \quad \text{(A14)}$$

where

$$J^0 = \int_0^\infty I^0(t)\, dt = \sum_k J_k^0 \quad \text{(A15)}$$

$$J = \int_0^\infty I(t)\, dt = \sum_k J_k \quad \text{(A16)}$$

Using this notation, Eqs. (A1) and (A4) may be rewritten in the form

$$I^0(t) = J^0 \sum_k f_k^0\, \phi_k^0(t) \quad \text{(A17)}$$

$$I(t) = J \sum_k f_k \phi_k(t) \quad \text{(A18)}$$

The fractions f_k can be expressed in terms of f_k^0 and Q_k. One can see from Eqs. (A13) and (A14) that

$$f_k = \frac{J^0}{J} \frac{f_k^0}{Q_k} \quad \text{(A19)}$$

After inserting Eq. (A19) into Eq. (A17), one obtains

$$I(t) = J^0 \sum_k \frac{f_k^0}{Q_k} \phi_k(t) \quad \text{(A20)}$$

where, based on Eqs. (A5) and (A11), the decay functions $\phi_k(t)$ may be written as

$$\phi_k(t) = \begin{cases} Q_k \dfrac{1}{\tau_k} e^{-t/\tau_k}, & 0 \le t \le t_d \\[2mm] [e^{t_d/\tau_k} - Q_k(e^{-t_d/\tau_k} - 1)] \dfrac{1}{\tau_k} e^{-t/\tau_k}, & t > t_d \end{cases} \quad \text{(A21)}$$

Equations (A20) and (A21) allow one to express the shape of the intensity decay of the fluorophore mixture as dependent on one general parameter, which is the time delay of the quenching pulse t_d, and three parameters for each fluorophore component, i.e., the mean fluorescence lifetime of the component τ_k, the steady-state fractional intensity of the component in the absence of light quenching f_k^0, and the amount of quenching of the component Q_k. The sum of the fractions f_k^0 is normalized to unity, so the number of independent parameters f_k^0 is equal to $n - 1$. For the one-beam light quenching the number of the parameters is reduced. First, in this case

$t_d = 0$, and second, for the one-beam light quenching the functions $\phi_k(t > 0)$ do not contain the parameters Q_k. Taking this into account, one of the parameters Q_k can be written before the summation sign in the Eq. (A20), showing that for this case the shape of the intensity decay of the mixture is described by $n - 1$ ratios Q_i/Q_k ($i \ne k$).

Measurement of the Extent of Light Quenching from the Frequency-Domain Intensity Decays

In frequency-domain analyses Eq. (A20) can be used to calculate (c) for each modulation frequency (ω) the two frequency-dependent quantities,

$$N_\omega = \int_0^\infty I(t) \sin(\omega t)\, dt$$

$$= J^0 \sum_k \frac{f_k^0}{Q_k} \int_0^\infty \phi_k(t) \sin(\omega t)\, dt \quad \text{(A22)}$$

$$D_\omega = \int_0^\infty I(t) \cos(\omega t)\, dt$$

$$= J^0 \sum_k \frac{f_k^0}{Q_k} \int_0^\infty \phi_k(t) \cos(\omega t)\, dt \quad \text{(A23)}$$

These quantities were then used to find the calculated phase angle ($\phi_{c\omega}$) and the calculated modulation ($m_{c\omega}$) of the emission

$$\phi_{c\omega} = \arctan(N_\omega/D_\omega) \quad \text{(A24)}$$

$$m_{c\omega} = \frac{1}{J}(N_\omega^2 + D_\omega^2)^{1/2} \quad \text{(A25)}$$

where the steady-state intensity J was calculated by integrating Eq. (A20) over time,

$$J = \int_0^\infty I(t)\, dt = J^0 \sum_k \frac{f_k^0}{Q_k} \quad \text{(A26)}$$

The best-fitted parameters, t_d, f_k^0, and Q_k, and goodness of fit were determined by the minimum value of

$$\chi_R^2 = \frac{1}{\nu} \sum_\omega \left[\left(\frac{\phi_\omega - \phi_{c\omega}}{\delta\phi}\right)^2 + \left(\frac{m_\omega - m_{c\omega}}{\delta m}\right)^2 \right] \quad \text{(A27)}$$

where ϕ_ω and m_ω are the experimental phase and modulation, respectively, $\delta\phi$ and δm are the experimental uncertainties, and ν is the number of degrees of freedom. Having found the best values of the parameters f_k^0 and Q_k, one can calculate the total amount of quenching Q
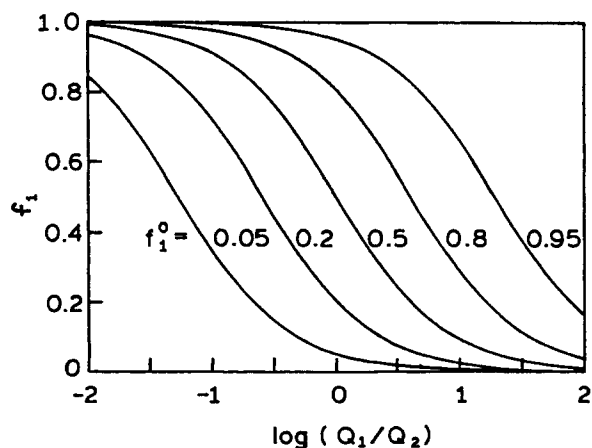
Fig. A1. Two-component mixture: influence of light quenching on the steady-state intensity fraction (f_1) of the first component for different values of the fraction (f_1^0) observed in the absence of light quenching. The independent variable is the ratio Q_1/Q_2 of the amounts of quenching of the respective components.
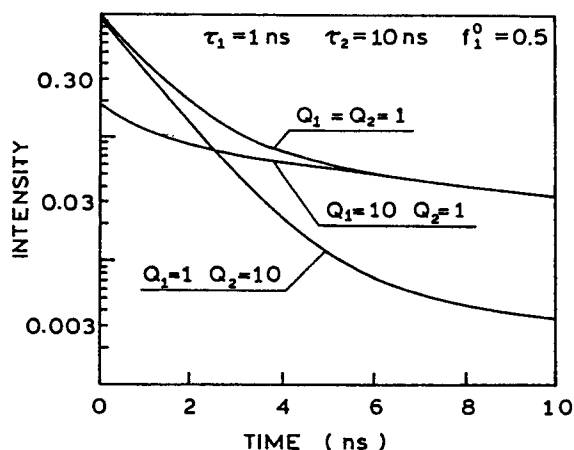

Fig. A2. Fluorescence decays of the two-component mixture in the presence of light quenching for different values of the amounts of quenching Q_1 and Q_2.

defined as

$$Q = \frac{J^0}{J} \qquad (A28)$$

and fractions f_k in the presence of light quenching [Eq. (A14)]. Equations (A28) and (A26) imply that

$$Q = \left[\sum_k \frac{f_k^0}{Q_k}\right]^{-1} \qquad (A29)$$

From Eqs. (A19), (A28), and (A29), one obtains

$$f_k = \frac{f_k^0}{Q_k} \left(\sum_k \frac{f_k^0}{Q_k}\right)^{-1} \qquad (A30)$$

In the case of two-species mixtures, $f_2 = 1 - f_1$ and Eq. (A30) simplifies to

$$f_1 = \left[1 + \left(\frac{1}{f_1^0} - 1\right)\frac{Q_1}{Q_2}\right]^{-1} \qquad (A31)$$

The dependence of f_1 on the ratio Q_1/Q_2 for different values of f_1^0 given by Eq. (A31) is shown in Fig. A1. It is seen that a significant change in the luminescence fraction f_1 may be achieved when the ratio Q_1/Q_2 is smaller than unity (for $0 \leq f_1^0 \leq 0.5$) or larger than unity (for $0.5 \leq f_1^0 \leq 1.0$). Note that in Fig. A1, $f_1 = f_1^0$ for $\log(Q_1/Q_2) = 0$. The strongest effect appears when the dominant fraction is quenched with a much higher efficiency than the other fraction.

One-Pulse Light Quenching of a Two-Component Mixture

If the excitation and quenching are caused by the same light pulse, then in the above equations the time delay t_d has to be set equal to zero. The decay function (A21) reduces to

$$\phi_k(t) = \frac{1}{\tau_k} e^{-t/\tau_k} \qquad (A32)$$

For the two-species mixture, using Eqs. (A20) and (A32) and taking into account that $f_2^0 = 1 - f_1^0$, one obtains for the intensity decay $I(t)$

$$I(t) = \frac{J^0}{Q_1} \left(\frac{f_1^0}{\tau_1} e^{-t/\tau_1} + \frac{Q_1}{Q_2} \frac{1 - f_1^0}{\tau_2} e^{-t/\tau_2}\right) \qquad (A33)$$

One can see from Eq. (A33) that the shape of the fluorescence decay in the presence of one-beam light quenching is not determined by the absolute values of the amounts of quenching Q_1 and Q_2, but by the ratio of these quantities Q_1/Q_2. However, the absolute values of both parameters, Q_1 and Q_2, still determine the observed absolute intensity of the fluorescence light.

Figure A2 shows the intensity decays calculated based on Eq. (A33) for $f_1^0 = 0.5$ and different values of the amounts of quenching Q_1 and Q_2. The decays are normalized so that $I(t = 0) = 1$ for $Q_1 = Q_2 = 1$. Equations (A32), (A22), and (A23) yield, for N_ω and D_ω,

$$N_\omega = \frac{J^0}{Q_1} \left[f_1^0 \frac{\omega\tau_1}{1 + \omega^2\tau_1^2} + \frac{Q_1}{Q_2}(1 - f_1^0)\frac{\omega\tau_2}{1 + \omega^2\tau_2^2}\right] \qquad (A34)$$

$$D_\omega = \frac{J^0}{Q_1} \left[f_1^0 \frac{1}{1 + \omega^2\tau_1^2} + \frac{Q_1}{Q_2}(1 - f_1^0)\frac{1}{1 + \omega^2\tau_2^2}\right] \qquad (A35)$$
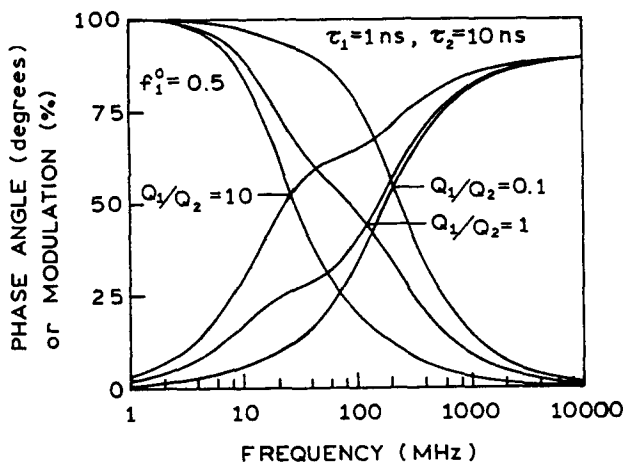
Fig. A3. Simulated frequency-domain responses for a two-component mixture in the presence of light quenching, predicted by Eqs. (A24)–(A26), (A34), and (A35) for $\tau_1 = 1$ ns, $\tau_2 = 10$ ns, $f_1^0 = 0.5$, and different values of the ratio of the amounts of quenching Q_1/Q_2.

Figure A3 shows the frequency-domain responses predicted by Eqs. (A24)–(A26), (A34), and (A35) for $\tau_1 = 1$ ns, $\tau_2 = 10$ ns, $f_1^0 = 0.5$, and different values of the ratio Q_1/Q_2. One notices that selective quenching of the long decay time ($Q_1/Q_2 = 0.1$) results in a shift of the frequency response to higher frequencies, due to the increased contribution of the $\tau_1 = 1$ ns component. The predicted fluorescence decays and/or frequency-domain responses may be compared with the experimental data. The lifetimes τ_1 and τ_2 are usually known from the independent measurements carried out on individual species in the absence of light quenching. The remaining two unknown parameters, f_1^0 and the ratio Q_1/Q_2, may be found from a global fit of the light quenched and unquenched data. It seems that such a global fit may even allow for evaluation of all four parameters τ_1, τ_2, f_1^0, and Q_1/Q_2, in the case when τ_1 and τ_2 are not known. Having estimated values of f_1^0 and Q_1/Q_2, one can calculate the fraction f_1 from Eq. (A31) and the fraction f_2 from the normalization relation $f_2 = 1 - f_1$. Because of the lack of the appropriate software, the above procedure has not been used in our calculations for evaluation of the ratio Q_1/Q_2. Instead, we first evaluated f_1^0, f_2^0, f_1, and f_2 and then calculated Q_1/Q_2 from Eq. (7).

If the directions of the absorption and emission dipoles are parallel, then the changes in the fraction f_1 (dependent on laser power) can be predicted based on Eq. (A31) and the expression for the amount of quenching Q_k obtained previously,[12]

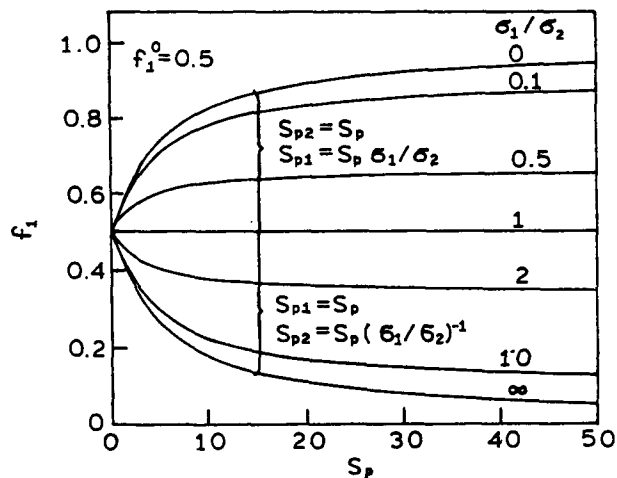$$Q_k = \left(\frac{3}{S_{pk}} \int_0^1 [1 - \exp(-S_{pk}x^2)] \, dx\right)^{-1} \quad (A36)$$

Fig. A4. One-pulse light quenching of the two-component mixture: dependence of the steady-state intensity fraction of the first component (f_1) on the ratio σ_1/σ_2 and parameter S_{p1} (for $\sigma_1/\sigma_2 \geq 1$) or S_{p2} (for $\sigma_1/\sigma_2 \leq 1$). The steady-state intensity fraction (f_1^0) of the component in the absence of light quenching is assumed to be equal to 0.5.

In Eq. (A36) the parameter S_{pk} is defined as

$$S_{pk} = W_p \sigma_k \quad (A37)$$

where W_p is the number of photons passing the unit area of the sample during a single pulse and σ_k is the light-quenching cross section of the kth species. For a given value of the cross section σ_k, the parameter S_{pk} is proportional to the laser power. Figure A4 shows the dependence of the steady-state fractional intensity of the first component [Eq. (A31)] on the ratio σ_1/σ_2 and parameter S_{p1} (for $\sigma_1/\sigma_2 \geq 1$) or S_{p2} (for $\sigma_1/\sigma_2 \leq 1$). It is assumed that the steady-state intensity fraction of the component in the absence of light quenching (f_1^0) is equal to 0.5. In the case where $\sigma_1/\sigma_2 \neq 1$ and the two species emit luminescence of different wavelengths, the color of the total luminescence emitted by the sample will be different for different powers of the excitation light.

Two-Pulse Light Quenching of the Two-Species Mixture

In the case where the luminescence of the two-component sample is excited by one pulse, quenched by the other pulse of a different wavelength, and delayed by the time t_d, Eqs. (A5) and (A20) yield

$$I(t) = \begin{cases} J^0 \left(\dfrac{f_1^0}{\tau_1} e^{-t/\tau_1} + \dfrac{1 - f_1^0}{\tau_2} e^{-t/\tau_2}\right), & 0 \leq t \leq t_d \\[2mm] J^0 \left(\dfrac{f_1^0}{\tau_1}(1 - q_1) e^{-t/\tau_1} + \dfrac{1 - f_1^0}{\tau_2}(1 - q_2) e^{-t/\tau_2}\right), & t > t_d \end{cases}$$
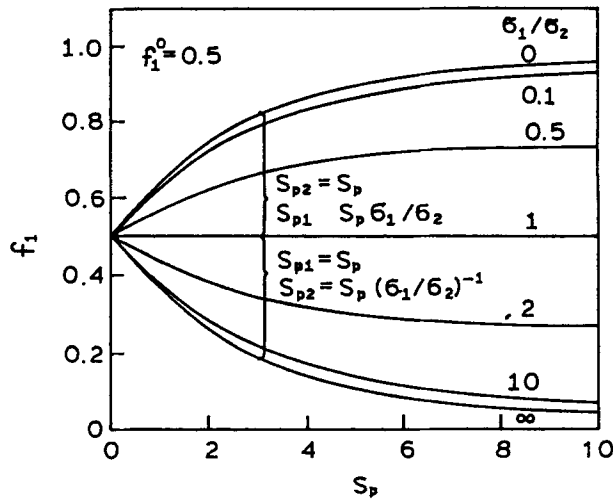
$$(A38)$$

Fig. A5. Two-pulse parallel light quenching of the two-component mixture: dependence of the steady-state intensity fraction of the first component (f_1) on the ratio σ_1/σ_2 and parameter S_{p1} (for $\sigma_1/\sigma_2 \geq 1$) or S_{p2} (for $\sigma_1/\sigma_2 \leq 1$). The steady-state intensity fraction (f_1^0) of the component in the absence of light quenching is assumed to be equal to 0.5.
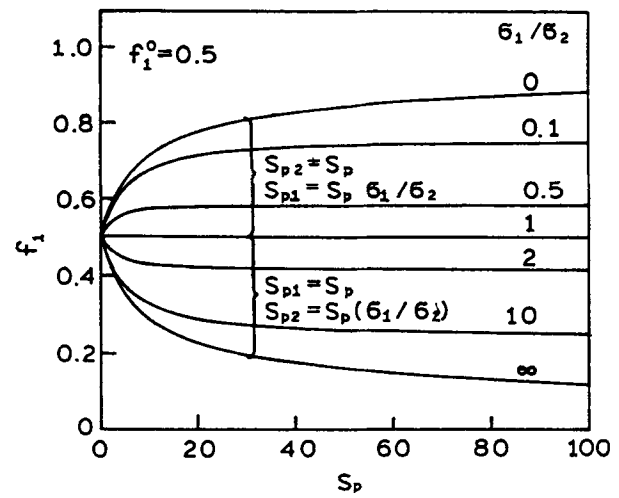

Fig. A6. Two-pulse perpendicular light quenching of the two-component mixture: dependence of the steady-state intensity fraction of the first component (f_1) on the ratio σ_1/σ_2 and parameter S_{p1} (for $\sigma_1/\sigma_2 \geq 1$) or S_{p2} (for $\sigma_1/\sigma_2 \leq 1$). The steady-state intensity fraction (f_1^0) of the component in the absence of light quenching is assumed to be equal to 0.5.

where q_1 and q_2 are related to the amounts of quenching Q_k by expression (12). Substituting Eq. (A38) into Eqs. (A22) and (A23), one obtains

$$N_a = J^0 \left\{ \frac{f_1^0}{1 + \omega^2\tau_1^2} \left[\omega\tau_1 - (\sin(\omega t_d) + \omega\tau_1\cos(\omega t_d))q_1 \, e^{-t_d/\tau_1}\right] \right.$$

$$\left. + \frac{1 - f_1^0}{1 + \omega^2\tau_2^2} \left[\omega\tau_2 - (\sin(\omega t_d) + \omega\tau_2\cos(\omega t_d))q_2 \, e^{-t_d/\tau_2}\right] \right\} \qquad (A39)$$

$$D_a = J^0 \left\{ \frac{f_1^0}{1 + \omega^2\tau_1^2} \left[1 - (\cos(\omega t_d) - \omega\tau_1\sin(\omega t_d))q_1 \, e^{-t_d/\tau_1}\right] \right.$$

$$\left. + \frac{1 - f_1^0}{1 + \omega^2\tau_2^2} \left[1 - (\cos(\omega t_d) - \omega\tau_2\sin(\omega t_d))q_2 \, e^{-t_d/\tau_2}\right] \right\} \qquad (A40)$$

In Eqs. (A39) and (A40) the values of the time delay t_d and lifetimes τ_1 and τ_2 are usually known. One can expect that for two-beam light quenching the global analysis of light-quenched and unquenched data may allow for simultaneous evaluation of the fraction f_1^0 and two amounts of quenching Q_1 and Q_2, contrary to the one-beam experiments, where f_1^0 and the ratio Q_1/Q_2 could be evaluated.

For $t_d = 0$ Eqs. (A38)–(A40) become identical to analogous expressions derived for one-pulse quenching [Eqs. (A33)–(A35)]. One can also see that setting $t_d = 0$ allows for the maximum effect of the two-pulse light quenching on the overall fluorescence decay, frequency-domain response, or steady-state fractions of fluorescence emitted by particular components. However, even for $t_d = 0$ the dynamics of changes of these quan-

tities with laser power will be different for two-pulse light quenching than for the one-pulse case. In these two cases the amounts of quenching Q_k depend in different ways on the parameters S_{pk}. Besides, in two-pulse light quenching the value of the parameter Q_k depends strongly on the relative polarization of the excitation and quenching beam. If the directions of the absorption and emission dipoles are parallel and the rotational motion of the molecules may be neglected, the following equation holds true [12]:

$$Q_k = \left\{ 1 - \exp\left(-\frac{t_d}{\tau_k}\right) \right.$$

$$\left. \left[1 - 3 \int_0^1 \exp(-S_{pk} \, x^2) \, x^2 \, dx\right]^{-1} \right\} \qquad (A41)$$

whereas for perpendicular light quenching, one has

$$Q_k = \left\{ 1 - \exp\left(-\frac{t_d}{\tau_k}\right) \left[1 - \frac{3}{2\pi} \int_0^{2\pi} \int_0^1 \exp \right. \right.$$

$$\left. \left. [-S_{pk}(1-x^2) \, \sin^2\varphi] \, x^2 dx \, d\varphi\right]^{-1} \right\} \qquad (A42)$$

The influence of laser power on the steady-state intensity fraction of the first component for parallel and perpendicular quenching and for different values of the ratio σ_1/σ_2 is shown in Figs. A5 and A6. In these figures t_d

= 0, and the independent variable is the parameter S_{p1} (when $\sigma_1/\sigma_2 \geq 1$) or S_{p2} (when $\sigma_1/\sigma_2 \leq 1$). It is evident that two-pulse parallel quenching changes the fraction f_1 most efficiently compared to one-pulse and two-pulse perpendicular quenching. Two-pulse perpendicular quenching is the least efficient way to change the fraction f_1.

REFERENCES

1. M. R. Eftink (1991) in *Topics in Fluorescence Spectroscopy, Vol. 2. Principles*, Plenum Press, New York, pp. 53–126.
2. M. R. Eftink (1991) in T. G. Dewey (Ed.), *Biophysical and Biochemical Aspects of Fluorescence Spectroscopy*, Plenum Press, New York, pp. 1–41.
3. E. Blatt and W. H. Saywer (1985) *Biochim. Biophys. Acta* **822**, 43–62.
4. M. R. Eftink, Ramsay, G. D. Ramsay, L. Burns, A. H. Maki, C. J. Mann, C. R. Matthews, and C. A. Ghiron (1993) *Biochemistry* **32**, 9189–9198.
5. J. Farinas, A. N. Van Hoek, L.-B. Shi, C. Erickson, and A. S. Verkman (1993) *Biochemistry* **32**, 11857–11864.
6. D. B. Calhoun, S. W. Englander, W. W. Wright, and J. M. Vanderkooi (1988) *Biochemistry* **27**, 8446–8476.
7. E. Blatt, A. Husain, and W. H. Sawyer (1986) *Biochim. Biophys. Acta* **871**, 6–13.
8. M. Punyiczki, J. A. Norman, and A. Rosenberg, (1993) *Biophys. Chem.* **47**, 9–19.
9. J. R. Lakowicz, I. Gryczynski, V. Bogdanov, and J. Kuśba (1994) *Photochem. Photobiol.* **60**, 546–562.
10. I. Gryczynski, J. Kuśba, and J. R. Lakowicz (1994) *J. Phys. Chem.* **98**, 8886–8895.
11. I. Gryczynski, J. Kuśba, Z. Gryczynski, H. Malak, and J. R. Lakowicz (1996) *J. Phys. Chem.* **100**, 10135–10144.
12. J. Kuśba, V. Bogdanov, I. Gryczynski, and J. R. Lakowicz (1994) *Biophys. J.* **67**, 2024–2040.
13. M. J. Cote, J. F. Kauffman, P. G. Smith, and J. D. McDonald (1989) *J. Chem. Phys.* **90**(6), 2865–2873.
14. Y. Chen, L. Hunziker, P. Ludowise, and M. Morgen (1992) *J. Chem. Phys.* **97**(3), 2149–2152.
15. V. E. Joos and M. Hauser (9192) *Arab. J. Sci. Eng.* **17**(2B), 209–217.
16. M. J. Rosker, M. Dantus, and A. H. Zewail (1988) *J. Chem. Phys.* **89**(10), 6113–6127.
17. J. L. Herek, S. Pedersen, L. Banares, and A. H. Zewail (1992) *J. Chem. Phys.* **97**(12), 9046–9061.
18. J. S. Baskin, L. Banares, S. Pedersen, and A. H. Zewail (1996) *J. Phys. Chem.* **100**, 11920–11933.
19. E. Gratton, J. R. Lakowicz, B. Maliwal, H. Cherek, G. Laczko, and M. Limkeman (1984) *Biophys. J.* **46**, 479–486.
20. J. R. Lakowicz, E. Gratton, G. Laczko, H. Cherek, and M. Limkeman (1984) *Biophys. J.* **46**, 463–477.
21. A. I. Butko, E. S. Voropai, V. A. Gaisenok, V. A. Saechnikov, and A. M. Sarzhevskii (1982) *Opt. Spectrosc. (USSR)* **52**(2), 153–156.
22. O. Svelto (1989) *Principles of Lasers*, Plenum Press, New York, pp. 52, 331.
23. I. Gryczynski, V. Bogdanov, and J. R. Lakowicz (1994) *Biophys. Chem.* **49**, 223–232.
24. J. R. Lakowicz, I. Gryczynski, V. Bogdanov, and J. Kuśba (1994) *J. Phys. Chem.* **98**, 334–342.
25. J. R. Lakowicz and B. P. Maliwal (1985) *Biophys. Chem.* **21**, 61–78.
26. G. Laczko, J. R. Lakowicz, J. Gryczynski, Z. Gryczynski, and H. Malak (1990) *Rev. Sci. Instrum.* **61**, 2331–2337.
27. R. F. Steiner and Y. Kubota (1983) in R. F. Steiner (Ed.), *Excited States of Biopolymers*, Plenum Press, New York, pp. 203–254.
28. D. Gloyna, A. Kawski, I. Gryczynski, and H. Cherek (1987) *Monatshefte Chem.* **118**, 759–772.